



MODELING AND EVALUATION OF INFRARED TRACKING SYSTEMS

Mohsen S. Aly*

ABSTRACT

The mathematical model of an infrared (IR) tracking system is developed. The system considered has a gyro-stabilized IR optical eye with rotating optical chopper. The dynamical equations of the gyro-mass assembly are derived. The equations that describe the signal processing in the electronic section of the system are obtained. Thus, the transfer functions that relates the precessional motion of the gyro assembly to the location of the IR-spot relative to the gyro spin axis are established. A physical simulation of the involved system is then presented. A digital controller is employed to control the operation of the simulated tracking loop. The control is achieved via the parallel interface bus (HP-IB). The chopping action of the gyro rotating reticle is physically simulated by placing an enlarged reticle in the front of an oscilloscope screen. The oscilloscope inputs are adjusted such that the oscilloscope spot traces a circle with angular frequency given by the gyro spinning speed. The electronic part of the tracking system is inserted in the simulation loop. This hardware-in-the loop procedure ensures that the simulation results are very close to reality. Via this simulation setup it is possible to develop and design the critical components of the system. In addition, the performance of the designed system can be tested. Simulation results show that the steady state tracking errors and the behavior of the tracking loop in the transient period are affected by the IR spot intensity and size in the reticle plane.

INTRODUCTION

The objective of an infrared tracking system is to provide information on the angular location of a real apparent infrared source of radiation. These information is usually in the form of estimates of the angular rates of the line of sight; i.e. the line in space joining the source center and the radiation aperture of the tracker. The tracking system has an optical axis which is the unique direction such that a fixed point source located in this direction produces the static equilibrium state of the tracking system.

In the closed-loop tracking system, the signal caused by the detected error angle actuates a derive servo mechnism to rotate the optical axis towards the line-of-sight. IR tracking systems that are involved in guided weapons are commonly known as IR seekers. The gyro-stabilized, solenoidal-torqued seeker is the most common structure. A magnetic dipole integral with the gyro rotor and detector assembly reacts with a control current which is passed through a solenoidal coil surrounding the gyro. The magnitude and phase of this precession current controls the magnitude and direction of the precession rate of the gyro rotor.

* Guidance Department, Military Technical College, Cairo, Egypt.

Thus, the directional information necessary for IR spot tracking is extracted primarily from the optical part of the seeker. Multidetector quadrant array may be utilized. In this case, the error signals are derived by mathematical manipulations of the separate detectors signals. There is another used configuration That utilizes single space- stabilized detector with rotating chopping disk called reticle. This type is widely used in the design of many tactical systems. The reticle pattern design is not straight forward and is-merely- governed by the system environmental conditions.

The rotating reticle can be viewed as a spatial filter. The fundamental objective of this filter is to highlight the salient dimensional or space features of a particular object-such as an airplane- at the expense of the dimensional detail received from undesired radiation-such as that received from clouds, horizons, lakes, etc [7]. To the author knowledge, very limited number of open archival literature discuss the modeling and evaluation of IR seekers. The dynamics of gyro- stabilized, solenoidal-torqued, quadrant detector seeker assembly had been investigated [4] and a simplified model had been derived. In this paper, the dynamical model of the gyro-stabilized, solenoidal torqued, seeker having rotating reticle and single detector is derived. It is assumed that a point target is located off-the boresight axis of the optical system. The considered rotating chopper configuration is such that the IR detector signal is amplitude modulated with the source position information being contained in the modulation signal. Thus, the modulating signal is used to control the orientation of the spinning mass so that the optical axis of the seeker follows the moving target. The equations that describe the operation of each subsystem in the IR tracking loop are constructed and the transfer function of the loop is then obtained. As well, a physical simulation setup is constructed to evaluate the effect of a large number of system parameters upon over-all performance of the seeker. The seeker components are broken up into subsystems in order to facilitate substitution of new reticle specimens and other optical parts. The optical subsystem is physically simulated by a rotating spot on the oscillograph CRT. The inertia of the rotating mass is represented by a low-pass-filter. The electronics of the seeker are inserted in the loop. A digital controller equipped with many interactive instruments is used to control the simulation loop components. There are two advantages for using a digital controller in the implementation. First, the development of precious function generators which are digitally controlled enables the accurate generation of the various signals with proper amplitudes and phases necessary for seeker circuits energization. Second, the presence

of control software makes it easy to vary the tracking loop parameters with minimum hardware modifications and observe the loop performance. Open loop gain is one of the parameters that can be varied easily via software.

INFRARED SEEKER DESCRIPTION

The conventional IR tracking system considered in the present work is comprised of five major subsystems; the optical telescope, reticle, detector, processing electronics, and the gyro-control electronics [3]. The optical telescope is of the cassagranian type. The infrared radiation from a source is collected by the primary mirror and together with intermediate optical elements, images the radiation onto the system focal plane. The focused radiation

is chopped by the rotating reticle and is then converted to electrical signals by the infrared detector. The electrical signal is processed by a set of electronics to enhance the signal-to-noise ratio and to define the target position within a given reference frame, thereby; providing a means to move the space stabilized homing eye.

Fig. 1 shows the commonly used optical part of the IR seeker. The primary mirror is also the inertial mass of the precessable free gyro. In addition, the mirror is a permanent magnet through which a precession torque can be generated to precess the optical platform. As shown in Fig. 1, energy from the target comes into the seeker through the hemispherical IR dome. The rays strike the primary mirror then the secondary mirror and are finally reflected through focusing lenses to the IR detector. In front of the detector is a reticle which, for center-null systems, modulates the incoming energy by spinning at the same frequency as the mirrors. It is this modulation that, when properly processed, permits the generation of a tracking error signal. It is noted that the spinning reticle is placed at the focal plane of the platform telescope with the optical axis aligned with the platform axis. A target off-boresight would traverse a circle on the reticle at a distance proportional to the angle of the target LOS off-boresight. The off-boresight target image would be chopped by the opaque/clear areas of the reticle to produce a carrier frequency that is 100 percent modulated by the spin frequency. The phase of the modulation signal relative to the spin drive reference is such that the precession torque moves the platform to place the target on the boresight. This phase is determined by the 50 percent transmission portion of the reticle.

The functional block diagram of the IR seeker is shown in Fig. 2. The rotor is surrounded by a precession solenoidal coil and two sets of pancake coils. The precession coil is used to control the orientation of the gyro rotor axis. One set of the pancake coils, together with the gyro rotor dipole, forms the torque motor that drives the rotor at constant speed. The other set of pancake coils detects the position of the rotor.

MATHEMATICAL MODEL OF THE IR TRACKING SYSTEM

Consider a two-dimensional object scene with a point source at \vec{r}_p . Let H_p [W/m^2] be the received irradiance at the optics from that point source. This source is imaged as

$$H_p \cdot f_o(\vec{r}_p), \quad (1)$$

where $f_o(\vec{r})$ represents the angular sensitivity function of the optics. In the image plane, there is a reticle which consists of adjacent opaque-transparent sectors. The reticle shape is given by the reticle function $f(\vec{r})$. The magnitude of f is between 0 and 1. The power incident on the IR detector can, thus, be written as

$$H(\vec{r}_p) = H_p \cdot f_o(\vec{r}_p) \cdot f(\vec{r}_p). \quad (2)$$

If the reticle is rotating with angular velocity ω_r , the detector signal is time varying. The incident power on the IR detector expressed in irradiance units will be

$$H(r_p, \theta_p, t) = H_p \cdot f_o(r_p, \theta_p) \cdot f(r_p, \theta_p - \omega_r t), \quad (3)$$

where r_p and θ_p are the polar coordinates of the source at the tip of the vector \vec{r}_p . The reticle function is periodic and can be represented as

$$f(r, \theta) = \sum_{\nu} \phi_{\nu}(r) e^{j\nu\theta}, \quad (4-a)$$

and

$$\phi_{\nu}(r) = \frac{1}{2\pi} \int_0^{2\pi} f(r, \theta) e^{-j\nu\theta} d\theta. \quad (4-b)$$

The peak value of ϕ_{ν} is at $\nu = \pm k$ since the reticle contains $2k$ opaque-transparent sectors. The IR detector signal can be written as

$$S(t) = S_p f_o(r_p, \theta_p) \sum_{\nu} \phi_{\nu}(r_p) e^{j\nu(\theta_p - \omega_r t)} \quad (5)$$

This signal is amplified in the carrier amplifier and then fed to a band-pass filter with frequency center $k\omega_r$ and band width $2m\omega_r$. The effect of the angular sensitivity function f_o and the intensity of the radiation source are eliminated by the action of the automatic gain control in the preamplification stages. Thus, the output of the filter will be

$$S(t) = S_o \Psi(r_p, \theta_p, \omega_r t), \quad (6)$$

where Ψ is defined as

$$\Psi(r_p, \theta_p, \omega_r t) = \sum_{\nu=k-m}^{\nu=k+m} e^{j\nu(\theta_p - \omega_r t)} \int_0^{2\pi} f(r_p, \theta) e^{-j\nu\theta} d\theta. \quad (7)$$

The shape of the considered reticle is such that the function Ψ is an amplitude modulated sinusoidal wave with the modulating signal amplitude being proportional to the deviation of the point source from the reticle center and phase being proportional to the direction of the point source relative to the seeker reference direction. Thus, the demodulation of the signal Ψ gives the precession signal voltage $v_p(t)$ as

$$v_p(t) = v_o(r_p) \sin(\omega_r t - \psi(\theta_p)) \quad (8-a)$$

The phase of v_p is measured relative to the reference signal given by

$$v_{ref}(t) = v_{ref} \sin(\omega_r t). \quad (8-b)$$

The precession signal is amplified in the precession amplifier and then used to drive the precession coil. The precession coil is an air-core solenoidal coil wound around the rotating gyro mass. Thus, it is almost purely resistive. The precession current will be

$$i_p(t) = i_o(r_p) \sin(\omega_r t - \psi(\theta_p)) \quad (9)$$

To obtain the equations of the precessional motion of the rotating mass, we will start with the following Euler's equation

$$\vec{T}_i = \left(\frac{d\vec{H}}{dt}\right)_i = \left(\frac{d\vec{H}}{dt}\right)_s + \vec{\omega} \times \vec{H} \quad (10)$$

Where \vec{H} is the total angular momentum of the seeker assembly and $\vec{\omega}$ is the angular velocity of the seeker assembly with respect to the inertial space. The subscript s denotes the seeker coordinate system and the subscript i denotes the inertial coordinate system as shown in Fig.3. \vec{T}_i is the inertial reaction torque. If we neglect the acceleration-induced pendulous torques, the damping and spring torques, the inertial reaction torque can be approximated by the magnetically induced torques \vec{T}_m . The angular velocity $\vec{\omega}$ can be written as

$$\vec{\omega} = \vec{\gamma} + \dot{\phi}\hat{i}_b + \dot{\theta}\hat{i}_y, \quad (11)$$

where $\vec{\gamma}$ is the total angular body rate of the vehicle. In the present simulation the body of the vehicle is stationary and thus $\vec{\gamma}$ is ignored. $\vec{\omega}$ is resolved in the seeker coordinate system as

$$\begin{aligned} \vec{\omega} &= \omega_s \hat{i}_s + \omega_a \hat{i}_a + \omega_b \hat{i}_b \\ &= \dot{\theta} \sin \phi \hat{i}_s + \dot{\theta} \cos \phi \hat{i}_a + \dot{\phi} \hat{i}_b \end{aligned} \quad (12)$$

The total angular momentum \vec{H} is expressed in the seeker coordinate system as

$$\vec{H} = \begin{pmatrix} I_s(\omega_s + \omega_r) \\ I_a \omega_a \\ I_b \omega_b \end{pmatrix} \quad (13)$$

The quantity $I_s \omega_r$ is the angular momentum of the spinning rotor, I_s , I_a , and I_b are the principle moments of inertia of the seeker assembly about the \hat{i}_s , \hat{i}_a , and \hat{i}_b axes, respectively, and ω_r is the rotor speed. The seeker under consideration is designed such that $I_s = I_a = I_b = I$ to eliminate the cross axis terms in Eq. 10. Combining Eqs. 12 and 13 yields

$$\left(\frac{d\vec{H}}{dt}\right)_i = I \begin{pmatrix} \ddot{\theta} \sin \phi + \dot{\theta} \dot{\phi} \cos \phi \\ \ddot{\theta} \cos \phi - \dot{\theta} \dot{\phi} \sin \phi + \dot{\phi} \omega_r \\ \ddot{\phi} - \dot{\theta} \omega_r \cos \phi \end{pmatrix}. \quad (14)$$

The magnetically induced torques will be first evaluated in the vehicle coordinate system, then transformed into the seeker coordinate system as

$$\vec{T}_m = (M)\vec{T}_M + \vec{T}_p, \quad (15)$$

where (M) is the transformation matrix between the seeker and vehicle coordinate systems and is given by

$$(M) = \begin{pmatrix} \cos \theta \cos \phi & \sin \phi & -\sin \theta \cos \phi \\ -\cos \theta \sin \phi & \cos \phi & \sin \theta \sin \phi \\ \sin \theta & 0 & \cos \theta \end{pmatrix}. \quad (16)$$

\vec{T}_M and \vec{T}_p are the spin motor torque and the precession torque; respectively. \vec{T}_M is acting along the \hat{i}_x direction. Define a coordinate system that rotates with the gyro rotor: \hat{i}_s , $\hat{i}_{a'}$, and $\hat{i}_{b'}$, such that the magnetic pole of the rotor is at the tip of the $\hat{i}_{a'}$ vector. At $t = 0$ $\hat{i}_a = \hat{i}_{a'}$. It can be shown that [4] the components of the unit vector $\hat{i}_{a'}$ projected into the vehicle coordinate system are

$$\hat{i}_{a'} = \begin{pmatrix} -\cos\omega_\tau t \sin\phi \cos\theta + \sin\omega_\tau t \sin\theta \\ \cos\omega_\tau t \cos\phi \\ \cos\omega_\tau t \sin\phi \sin\theta + \sin\omega_\tau t \cos\theta \end{pmatrix}. \quad (17)$$

The rotor is assumed to be within a uniform solenoidal magnetic field with normalized flux-density vector $\vec{B}_p = B_p \hat{i}_x$. The precession torque will be

$$\vec{T}_p = 2\vec{B}_p \times \hat{i}_{a'} \quad (18)$$

The induced magnetic flux density vector is in time phase with the precession current given by Eq. 9. It should be noted that there is an additional current induced in the precession coils due to the rotation of the magnetized rotor. This induced current gives rise to an additional torque; however, it will be neglected in the present context. Thus,

$$B_p(t) = B_o(r_p) \sin(\omega_\tau t - \psi(\theta_p)) \quad (19)$$

Combining Eqs. 15 to 19, the total magnetic torque projected in the seeker coordinate system will be

$$\vec{T}_m = (M) \cdot \begin{pmatrix} \vec{T}_M \\ -2B_p(t)(\cos\omega_\tau t \sin\phi \sin\theta + \sin\omega_\tau t \cos\theta) \\ 2B_p(t)(\cos\omega_\tau t \cos\phi) \end{pmatrix} \quad (20)$$

The terms with frequency $2\omega_\tau$ will be neglected since the frequency $2\omega_\tau$ lies outside the bandwidth of the dynamics of the system. Thus, Eq. 20 is reduced to

$$\vec{T}_m = \begin{pmatrix} T_M \cos\theta \cos\phi + a \sin\phi - b \sin\theta \cos\phi \\ -T_M \cos\theta \sin\phi + a \cos\phi + b \sin\theta \sin\phi \\ T_M \sin\theta + b \cos\theta \end{pmatrix}, \quad (21)$$

where a and b are given by

$$a = -B_o(r_p)(\cos\theta \cos\psi - \sin\theta \sin\phi \sin\psi),$$

and

$$b = -B_o(r_p) \cos\phi \sin\psi.$$

The seeker head is operating within a narrow cone; therefore, the use of small-angle approximation appears justified. Also, small higher order terms are neglected. The inertial reaction torque equation can be written as

$$\begin{pmatrix} T_M - B_o \phi \cos \psi + B_o \theta \sin \psi \\ -T_M \phi - B_o \cos \psi \\ T_M \theta - B_o \sin \psi \end{pmatrix} = I \cdot \begin{pmatrix} \ddot{\theta} \phi + \dot{\theta} \dot{\phi} \\ \ddot{\theta} - \dot{\theta} \dot{\phi} \phi + \omega_\tau \dot{\phi} \\ \ddot{\phi} + \omega_\tau \dot{\theta} \end{pmatrix}. \quad (22)$$

The spinning frequency ω_τ is very large compared with $\dot{\theta}$ and $\dot{\phi}$. Also, $\omega_\tau \dot{\phi}$ and $\omega_\tau \dot{\theta}$ are large compared with $\ddot{\theta}$ and $\ddot{\phi}$; respectively. By taking the Laplace transform of Eq. 22, one can get the following transfer functions:

$$\theta = \frac{B_o(r_p) \cdot \sin \psi}{s(T_M + I\omega_\tau s)} \quad (23 - a)$$

and

$$\phi = \frac{-B_o(r_p) \cdot \cos \psi}{s(T_M + I\omega_\tau s)} \quad (23 - b)$$

Thus, the instantaneous direction of the spinning axis can be obtained in terms of the precession voltage. These relations are greatly useful in that, the performance of the seeker electronics modules can be tested without spinning up its gyro which keeps the gyro life time during the development and test phases.

PHYSICAL SIMULATION

The simplified physical simulation block diagram of the IR tracking loop is shown in Fig. 4. A digital controller is employed to control the operation of the seeker stimuli generators. The detailed description of the setup is found in [9]. The output from the stimuli generators simulates the real signal obtained from a stabilized detector. This output is fed to the seeker electronic circuits. The output of the seeker precession amplifier (defined by Eq.8-a), which represents the targets polar error, is resolved by multiplying it with the reference sine and cosine signals. The output of the analog multipliers are filtered by the low-pass-filters which simulates the gyro mass. The outputs of the filters, thus, represent the precession speeds $\dot{\theta}$ and $\dot{\phi}$ of the IR eye along two perpendicular directions in the lateral plane. These outputs are acquired instantaneously and are used to update the gyro spinning axis direction.

The experiment is started by a given target off-the gyro axis which corresponds to IR spot on the reticle plane away from the reticle center. According to the IR spot location, the controller instructs the stimuli generators to produce the proper input signals to the seeker electronics. The output of the seeker is resolved, filtered, and fed back to the controller. The control software modifies the position of the gyro axis relative to the target according to the acquired seeker output. The process continues until the target spot moves to the reticle center which means that the gyro axis moves to the target LOS.

SIMULATION RESULTS

The tracking process is initiated by assuming the presence of an IR spot near the reticle circumference (T_o), as shown in Fig. 5. Simulation results show that the IR spot size in the reticle plane relative to the width of the opaque-transparent sectors and the spot intensity critically affect the transient and steady state performance of the tracking loop. After closing the tracking loop, the IR spot moves toward the reticle center and keeps wandering around it. The average distance between the instantaneous spot locations and the reticle center represents the steady state tracking error of the tracking loop. The trajectory shape from the initial target position T_o to the steady state position describes the tracking loop transient behavior. Inspection of the obtained results reveals that the increase spot intensity improves both the transient and steady state responses of the tracking loop. However, increasing the IR spot size will increase the tracking errors. Thus, the focusing accuracy of the seeker optical eye highly affects the tracking accuracy which imposes a stringent condition on the useful operating band of frequencies of the seeker.

CONCLUSIONS AND FUTURE WORK

The mathematical model of the IR seeker having a rotating chopper is developed. The bandwidth of the seeker tracking loop is obtained in terms of the dynamical parameters of the spinning gyro mass. The model is supported by a digitally controlled physical simulation setup which enables testing the performance of the tracking loop. Steady state tracking errors or the tracking accuracy and The behavior of the tracking loop in the transient period are investigated as well. Building the main guidance loop with the present technique represents a challenging future research point.

REFERENCES

- [1] E. J. Eichblatt, Jr. and A. Pgnataro, "Test and Evaluation of the Tactical Missile," Ed. Emil J. Eichblatt, Jr. , Pacific Missile Test Center, California, Library of Congress, 1989.
- [2] H. F. Meissinger, "Simulation of Infrared Systems," *Proceeding IRE*, vol. 47, pp 1586-1592, September 1959.
- [3] J. J. May, Jr. and M. E. Van Zee, "Electro-Optic and Infrared Sensors," *Microwave Journal*, September 1983.
- [4] S. A. White, "Dynamics of Solenoidal-Torqued Gyro-Stabilized Seeker Assembly for Guidance and Tracking," *IEEE Trans. Aerospace and Electronics Systems*, vol. AES-10, pp. 113-122, January 1974.
- [5] P. Zarchan, "Tactical and Strategic Missile Guidance," A. Richard Seebass, Library Congress, 1990.
- [6] P. C. Cregory, "Guidance Simulation Techniques," AGARD lecture series no 101 on guidance and control for tactical weapons with emphasis on simulation and testing, June 1979.
- [7] A. F. Nicholson, "Error Signals and Discrimination in optical Trackers that See Several Sources," *Proceeding of the IEEE*, pp. 56-69, January, 1965.

- [8] D. D. Moerder, A. J. Calise, and P. Clemmon, "Optimal Open Multistep Discretization Formulas for Real-Time Simulation," *J. of Guidance, Control, and Dynamics*, vol. 6, May-June 1993, pp. 557-563.
- [9] Mohsen S. Aly, "Real-Time Simulation of Gyro-Stabilized, Infrared Tracking Seeker," Al-Azhar Engineering Third International Conference, Cairo, Egypt, pp. 531-542, December 1993.

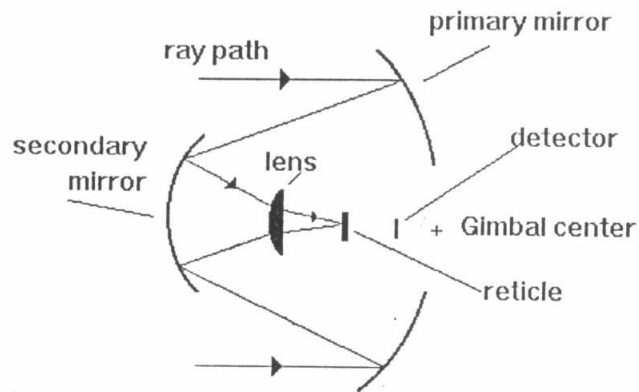


Fig. 1. Infrared Red Optical Eye.

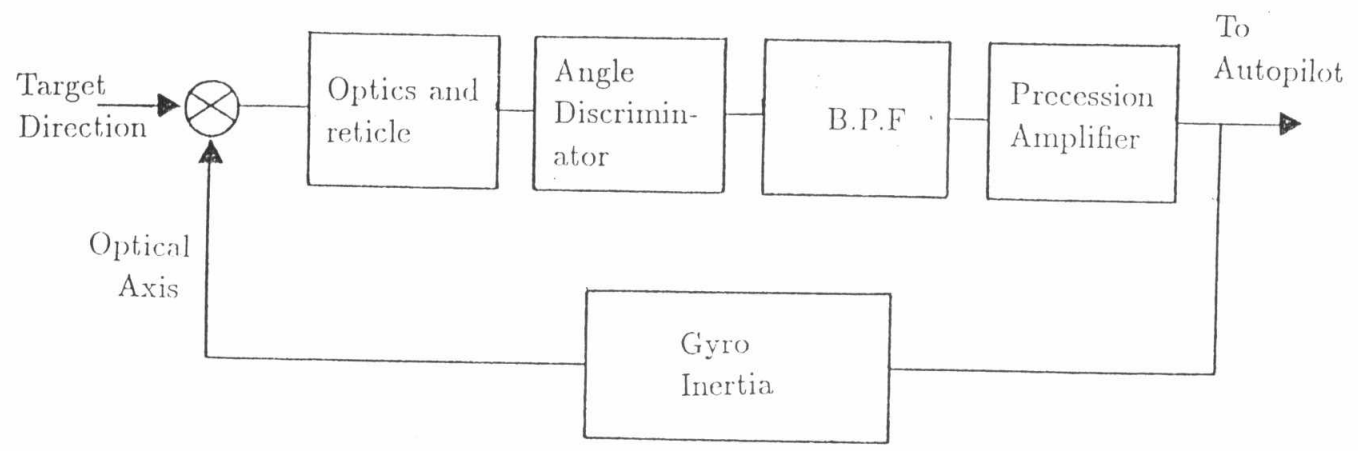


Fig. 2. Functional Block Diagram of IR-Seeker.

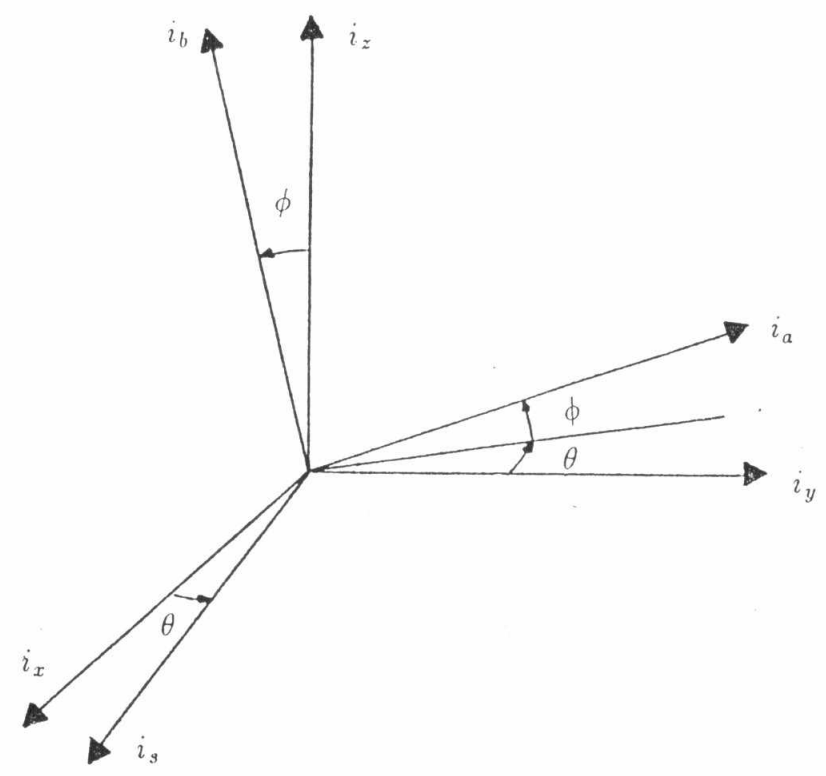


Fig. 3. Inertial and Seeker Coordinate Systems.

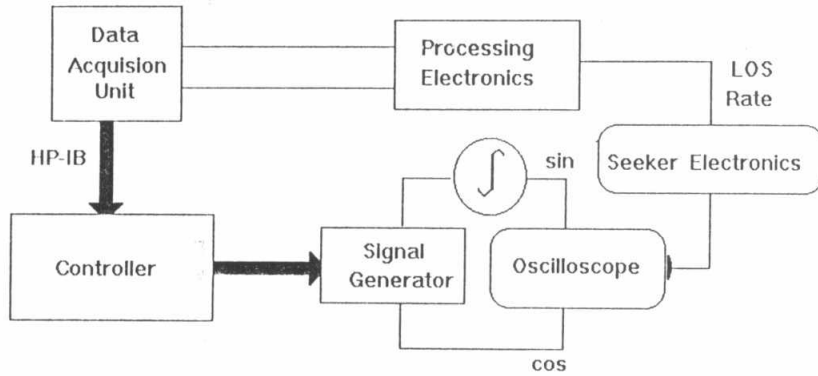


Fig. 4. Physical Simulation Block Diagram Of IR Tracking Loop

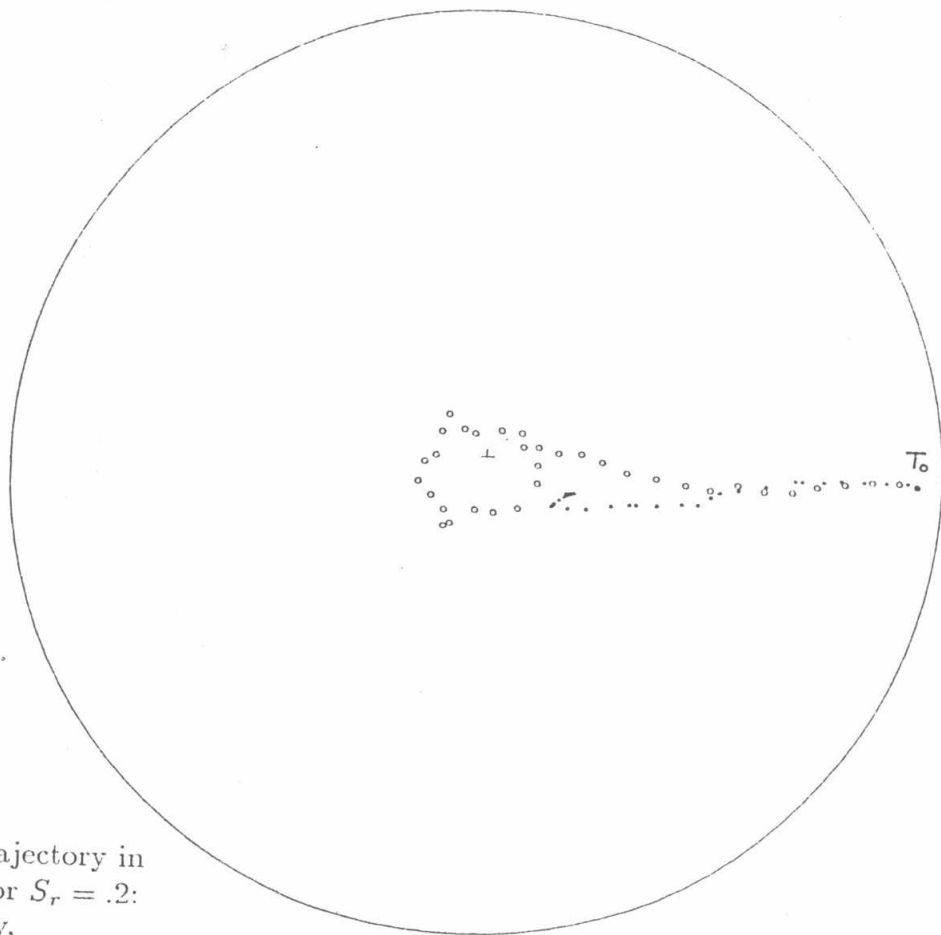


Fig. 5. IR spot trajectory in the reticle plane for $S_r = .2$:
 . . . High intensity,
 o o o Low intensity.